Retinal Fundus Image Enhancement using Piecewise Gamma Corrected Dominant Orientation based Histogram Equalization

P. Sujith Reddy, Himanshu Singh, Anil Kumar, L. K. Balyan and Heung-No Lee

***Abstract*—Retinal fundus images play an essential role in the diagnosis of retina-related diseases and hence, their quality enhancement is essential for doctors to make a reliable clinical diagnosis. This paper presents an advanced retinal fundus image enhancement method by employing an efficiently modified and biologically inspired levy-flight firefly optimizer in association with a novel optimally weighted piecewise gamma corrected energy redistributed dominant orientation based texture histogram equalization framework for imparting overall quality improvement of retinal fundus images. The key intelligence is to utilize a weighted summation of intensity as well as texture based enhancement along with an efficiently defined cost function. The cost function has been framed such that more and more intensity span can be explored in a positive manner. Rigorous experimentation by employing the performance evaluation and comparison with recently proposed enhancement approaches so that the explicit outperformance can be underlined.**

Index Terms*—Retinal fundus imaging; piecewise gamma correction; cuckoo search optimization; quality enhancement.

I. Introduction

DIGITAL imagery and its various forms aggregate the core basis for digital information era. Day-by-day increasing audacious happenings and corresponding revolutionary improvements in any sphere of science and technology cannot be imagined without digital imaging techniques in one form or the other. It grants much wider range of algorithms to be applied to the input data and can avert many disputes [1]. Despite of surprising advancements for image capturing devices, still there are various natural as well as artificial artifacts, which lead to poor quality of the image captured, and hence, quality improvement for raw captured images is an indispensible part of pre-processing of the images [2]. Retinal fundus imaging provides rich information of pathological changes those are usually with sporadic illumination, low contrast and blur of the details due to the complex imaging environments [3]. Retinal imaging is an important and effective tool for screening retinal diseases such as Diabetic Retinopathy (DR), Glaucoma, hypertension, stroke, and age-related Macular Degeneration (AMD) and Cardiovascular disease.

P. Sujith Reddy, Himanshu Singh, Anil Kumar and L. K. Balyan are with Indian Institute of Information Technology Design and Manufacturing, Jabalpur-482005, India (E-mail: himanshu.iiitj@ieee.org;{sujithreddy2502; anilkdee; lokendra.balyan}@gmail.com).

Heung-No Lee is with Gwangju Institute of Science and Technology, Gwangju, South Korea. (E-mail: heungno@gist.ac.kr).

As a standard image modality, fundus camera is usually used to acquire retinal images, showing structure like optical disc, retinal vessels and several others [4]. The changes detected in these structures can be As a standard image modality, fundus camera is usually used to acquire retinal indications of a pathological condition associated with diseases such as glaucoma and diabetic retinopathy, which can further be confirmed by performing detailed analysis of these retinal mages [5]. The main intention of this enhancement method is to correct the contrast and highlight the retinal vessels. Therefore the analysis of retinal images is an important and helpful diagnostic tool. In fact, the analysis of retinal images can also render beneficial to the classification of the disease stages, on identifying the underlying problem. In various domains of engineering and technology, image processing is in very high demand, both for human vision as well as machine vision perspective. Some of the retinal images are clinically unacceptable due to eye lesions and imperfect imaging techniques which include exudates, hemorrhages, opacity of refractive media and patient's eye movement. Irregular blurring, illumination, low contrast and imprecise focus truncate the aspect of retinal images, emerging in loss of sensitivity and specificity for diagnostic scope. It may also prejudice ophthalmologists' capability to enact significant eye features or categorize retinal diseases. Retinal images which are of poor quality make it difficult for consequent authentic segmentation and computer-aided diagnosis of retinal related diseases, which can be used to automate the disclosure process and to assist ophthalmologists. Thus, it is significant to overcome the objections associated with poor quality retinal images [6]. Wide variety of histogram based and transform-domain based techniques have already been available in literature for general images [5-6]. First, general histogram equalization (GHE) approach [7] was initially introduced, thereafter its various variants have been proposed by many researchers. In the same context, requirement of localized processing seems more ambitious and hence various sub-equalization motivated histogram based enhancement approaches have also been contemplated. A detailed literature analysis in this ambience is also available in [5-6]. Momentous contributions like contrast-limited adaptive HE also dragged the core attraction of the researchers. Statistical segmentation based sub-equalization like median-mean based sub-image clipped HE (MMSICHE) [8] has also been introduced. Afterwards, the averaging histogram equalization (AVGHEQ) [9], HE based optimal profile compression (HEOPC) [10] method for color image enhancement followed by HE with

978-1-5386-3520-9/18/$31.00 ©2018 IEEE

maximum intensity coverage (HEMIC) [11] were proposed. Also, the adaptive gamma correction with weighting distribution (AGCWD) [12] and its productive variations [13-17] were proposed for dark images. Eventually, the intensity and edge based adaptive unsharp masking filter (IEUMF) [18] based enhancement has been proposed by operating the unsharp masking filter for edge enhancement followed by the significant proposal of dominant orientation-based texture histogram equalization (DOTHE) [19] especially of textural improvement. In this paper, the piecewise gamma correction is optimally associated with energy redistributed texture-orientation dominance framework for transmitting intensity as well as for the texture based quality enhancement approach and is employed for optimal enhancement of dark images. Remaining content is organized as: Section II which deals with the problem formulation followed by the proposed methodology. Experimentation is discussed in Section III and finally, conclusion is drawn in Section IV.

II. Proposed Methodology

Parallel band processing is generally required for multiband images, but for enhancing equivalent color images Hue-Saturation-Intensity (HSI) model can be applied to decouple the chromatic and non-chromatic information content, as [1]:

$$\left[H(m,n),S(m,n),I(m,n)\right]^T = T_{RGB}^{HSI}\left[R(m,n),G(m,n),B(m,n)\right]^T, \quad (1)$$

Here, T_{RGB}^{HSI} is *RGB* to *HSI* transformation process. The color image enhancement can be done by upgrading only the brightness intensity values, keeping rest (hue and saturation) values preserved, followed by linear stretching. The gamma compressed interim intensity channel can be evaluated as [1]:

$$I_{gcp} = \left(I_{in}\right)^{\gamma}, \qquad \gamma>1, \quad (2)$$

The corresponding gamma expanded interim intensity channel can be evaluated as [1]:

$$I_{gex} = \left(I_{in}\right)^{1/\gamma}, \qquad \gamma>1, \quad (3)$$

Later on, evaluation for third interim channel can be done by identifying the tile-wise texture dominance followed by variance based thresholding (for separate identification of smooth as well as non-smooth patches). For this purpose, the entire image is sectioned into tile-wise collection of several 5×5 (or any odd-ordered) sized patches. These extracted patches are divided into smooth or rough by implanting a variance threshold τ on each image patch. Further, the rough patches are classified into dominant or non-dominant orientation patches by reckoning their local orientation which is based on singular value decomposition (SVD) of the gradient vectors of the patch. The procedure required for categorizing the rough patch into dominant or non-dominant orientation patches and the method to construct the histogram is highlighted below. The local estimate of gradient $\nabla I(m,n)_i$ at each pixel (m,n) in patch is calculated as:

$$\nabla I(x,y)_i = \left\{\frac{\partial I(x,y)}{\partial x}, \frac{\partial I(x,y)}{\partial y}\right\}, \quad (4)$$

Collectively for N patches, the gradient map can be framed as:

$$GM = \left\{\nabla I(x,y)_1, \nabla I(x,y)_2, \nabla I(x,y)_3, \ldots, \nabla I(x,y)_N\right\}^T, \quad (5)$$

Next, SVD of the gradient map is computed.

$$\Psi = U\Sigma V^T \quad (6)$$

Where $U \in R^{n\times n}$ represents the contribution of each vector to the corresponding singular vector; $\Sigma \in R^{n\times 2}$ represents the energy in the dominant directions; and $V \in R^{2\times 2}$ represents the orientation. In matrix V, the dominant and the subdominant orientations of the gradient field are represented by the columns v_1 and v_2 respectively. The dominant measure D divides the rough patches into dominant and non-dominant orientation patches, which can be calculated by:

$$D = \frac{\left(\Sigma(1,1) - \Sigma(2,2)\right)}{2}, \quad (7)$$

In the above equation, $\Sigma(1,1)$ and $\Sigma(2,2)$ are singular values representing the energy in the dominant direction. The patches having dominant measure lesser than the significance level threshold D' contains no dominant orientation as they are only pure white noise. The patches which have dominant measure greater than the significance level threshold D' are dominantly oriented. Now, the intensity distribution (histogram) of the texture patches is computed. All the intensities present in the texture patches are required for histogram formation. Further, Cumulative Density Function (CDF) is used to map the input image histogram into new dynamic range. Locations of various local maxima values have to be observed and accordingly admissible sub-histograms can be derived. Individual CDFs are evaluated for all the sub-histograms as:

$$c_j(i) = \frac{1}{N_j}\sum_{k=0}^{i} h_j(k), \quad (8)$$

Here, N_j is the net pixel-count in j^{th} sub-histogram (corresponding to the j^{th} patch). Equalize all the j sub-histograms autonomously as:

$$\tilde{I}_j = I_{j\_min} + \left(I_{j\_max} - I_{j\_min}\right) * c_j(i), \quad (9)$$

Access the overall equalized image as:

$$I_{tex\_dom} = \bigcup_{\forall m} \tilde{I}_m, \quad (10)$$

Now, the weighted summation input intensity channel with uniformly equalized intensity channel $\left(\hat{I}_{en}\right)$ can be obtained as-

$$\hat{I}_{en} = \left(\frac{\alpha}{1+\beta}\right) I_{gcp} + \left(\frac{1-\alpha}{1+\beta}\right) I_{gex} + \left(\frac{\beta}{1+\beta}\right) I_{tex\_dom}, \quad (11)$$

Here, unfortunately over-ranging may get resulted, and it should be minimized efficiently without affecting the resulted enhancement and hence it can be included as a penalty term in the cost function framed here, as:

$$J = H.\Delta\sigma^2.\left(\frac{\sigma^2}{\mu}\right).\left(1 - \frac{n_{ov}}{M*N}\right), \quad (12)$$

Here, $\mu, \sigma^2, \Delta\sigma^2$ *and* H stands for output brightness, contrast, relative contrast, and output Shannon entropy, respectively for an L-bit, $M*N$ image. Here, n_{ov} is the count of the normalized over-ranged pixels, which can be evaluated as:

$$n_{ov} = \sum\left\{\tilde{I}_{mn} < 0 \cup \tilde{I}_{mn} > 1\right\}, \quad (13)$$

Here, $\hat{h}(i)$ stands for histogram of the processed image. Cost-function is devised here, so that the relative variance along with maximal information restoration can be imparted with proper check on relative mean brightness. Biologically inspired and later on efficiently modified CSOA is employed for optimal enhancement for dark images, by efficient exploration followed by generous exploitation in a three-dimensional search space so that the required optimal values for $\alpha, \beta,$ and γ can be obtained. The efficient parametric variation for framing search space derived analytically is $[\alpha, \beta, \gamma] \leftarrow [(0,1),(0,5),(1,5)]$. Combative psychology of the cuckoo bird, and its interesting breeding behavior (more precisely, its brood parasitism) fascinated various researchers to frame an analogously designed population oriented metaheuristic optimization algorithm. CSOA is highly perceptible for determining multimodal, multi-objective, and highly non-linear optimization issues deprived of any kind of comprehensive search. Core structure for CSOA and its problem solving approach in its original form has been already detailed in [20]. Following the Levy distributed quasi-random flight; a suitable intelligence has been also introduced, where the prevailing step has to be decided by keeping "current location" and "next-state transition probability" in the mind. This type of step flight pattern is highly compatible and beneficial with CSOA behaviour. Simplified analogous demeanoral modelling has been done by establishing three rules, as already existed in the admissible literature. Levy distributed flight is generally for both local as well as global analysis of the corresponding search space. Levy flight for iterative new solution x^{t+1} for the i^{th} cuckoo can be forged as:

$$x_i^{t+1} = x_i^t + \partial \oplus L\acute{e}vy(\beta), \quad where,\ \partial > 0, \tag{14}$$

Here, entry-wise walk during multiplications can be determined through product operation $\oplus$. Random exploration follows Levy distributed (having both first as well as second moment infinite) random step size, as [20]:

$$L\acute{e}vy: \ u = t^{-\lambda}, \qquad \forall\ \lambda \in (1,3], \tag{15}$$

This power law step-flight assigned random walk leads to the introduction of few new solutions in the proximity of best solution (identified so far), and in this manner local search can be boosted up. In addition, a benevolent share of new solutions should be created through far-field randomization, so that the local deceiving can be avoided and global inspection can be renewed. Finally, enhanced channel is obtained and hence, correspondingly enhanced color image can be derived as:

$$\left[\hat{R}(m,n), \hat{G}(m,n), \hat{B}(m,n)\right]^T = T_{HSI}^{RGB}\left[H(m,n), S(m,n), \hat{I}(m,n)\right]^T, \tag{16}$$

Here, T_{HSI}^{RGB} is *HSI* to *RGB* transformation process.

III. Experimentation and Result Analysis

A. Assessment Criterion

Comparative evaluation is performed qualitatively for resultant images [21] and for further quantitative assessment, performance metrics such as brightness (B), contrast/variance (V), entropy (H), sharpness (S), and colorfulness (C) are derived here.

B. Qualitative Assessments

Reimplementation for various recent state-of-the-art methodologies (namely, GHE, ADAPHE, AGCWD, and HEOPC) has been done. Visual results for enhanced images are presented in Fig. 1.

TABLE I

QUANTITATIVE EVALUATION WITH COMPARISON AMONG GHE [7], ADAPHE [3], AGCWD [12], HEOPC [10], AND THE PROPOSED APPROACH USING METRICS TERMED AS BRIGHTNESS, CONTRAST, ENTROPY, SHARPNESS AND COLORFULNESS.

S. No.	INDICES	INPUT	GHE	ADAPHE	AGCWD	HEOPC	OURS
1.	Brightness	0.6368	0.5497	0.6545	0.7273	0.5764	**0.6545**
	Contrast	0.068	0.1223	0.0694	0.0528	0.0889	**0.0694**
	Entropy	5.6271	5.1901	5.7954	5.7838	5.5716	**5.912**
	Sharpness	0.0802	0.1535	0.1904	0.1186	0.102	**0.1904**
	Colorfulness	0.2827	0.2551	0.3082	0.3746	0.2441	**0.3899**
2.	Brightness	0.6921	0.5462	0.6859	0.764	0.6949	**0.6859**
	Contrast	0.0598	0.1208	0.0709	0.0528	0.0597	**0.0709**
	Entropy	5.6508	4.9697	5.7605	5.7137	5.7504	**5.8098**
	Sharpness	0.102	0.1217	0.199	0.1178	0.1086	**0.199**
	Colorfulness	0.3722	0.275	0.3772	0.4473	96.3018	**0.4446**
3.	Brightness	0.7191	0.549	0.7026	0.7882	0.6756	**0.7026**
	Contrast	0.0467	0.122	0.0595	0.0398	0.0617	**0.0595**
	Entropy	5.6671	4.9553	5.7758	5.75	5.7236	**5.8308**
	Sharpness	0.0747	0.1204	0.1626	0.0898	0.0909	**0.1626**
	Colorfulness	0.3934	0.2815	0.3881	0.4688	91.8551	**0.4609**
4.	Brightness	0.6562	0.5466	0.6707	0.7332	0.6637	**0.6707**
	Contrast	0.0744	0.1207	0.0737	0.0658	0.0708	**0.0737**
	Entropy	4.5803	4.0234	4.6757	4.6092	4.6801	**4.6893**
	Sharpness	0.095	0.1029	0.1849	0.1068	0.0972	**0.1849**
	Colorfulness	0.3903	0.3079	0.4081	0.4824	103.0327	**0.492**

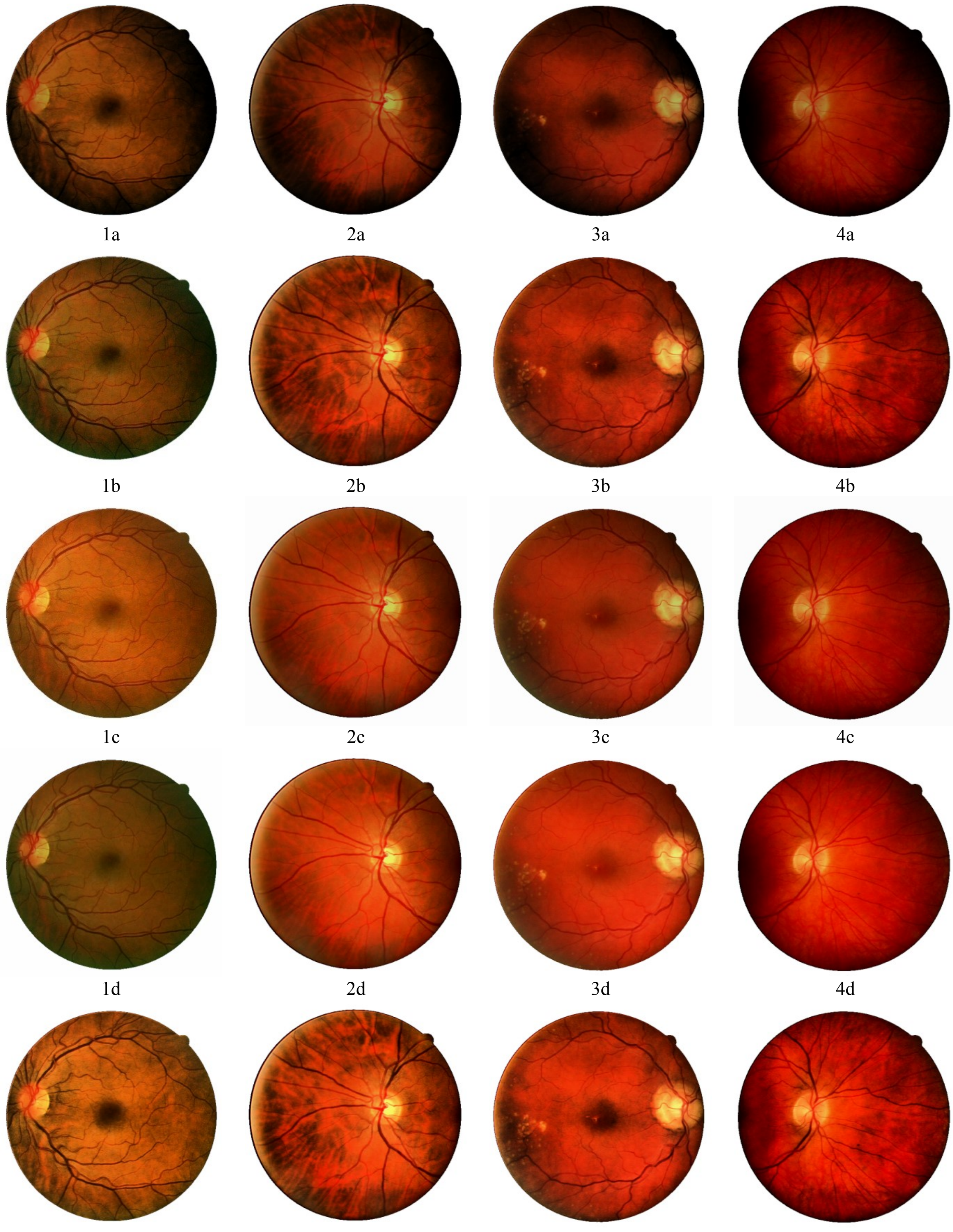

Fig. 1. Visual evaluation with comparison among 1a-4a: GHE [7]; 1b-4b: ADAPHE [3]; 1c-4c: HEOPC [10]; 1d-4d: AGCWD [12]; and 1e-4e: the proposed approach.

C. Quanitative Assessments

For explicit quantitative comparison and evaluation, relevant performance metrics have been evaluated and listed in Table I.

IV. Conclusion

As a concluding remark, it can be explicitly identified that the prospective path will be highly suitable for overall quality enhancement of retinal fundus images and hence directly helps the radiologists in various kinds of medical diagnosis as well as early detection of symptoms of retinal disorders. Especially when followed by segmentation and further by classification the quality enhanced fundus images outperforms for medical diagnostic purposes. The dominant texture-orientation based equalization when associated with the recently proposed piecewise gamma corrected weighted summation framework, yields highly appreciable results when intuitively governed by highly efficient exploration as well as exploitation following the biologically inspired cuckoo search optimization (CSO). Although the approach is some-how iterative, but the associated robustness and it's highly flexible behavior counter-balances for that. Highly consistent performance metrics are examined for proper image quality evaluation and accordingly, the outperformance of the proposed framework can be easily highlighted in addition to the qualitative evaluation through visual results.

References

[1] P. Dai, H. Sheng, J. Zhang, L. Li, J. Wu, and M. Fan, "Retinal Fundus Image Enhancement Using the Normalized Convolution and Noise Removing," *Int. J. Biomed. Imaging*, vol. 2016, 2016.

[2] M. Zhou, K. Jin, S. Wang, J. Ye, and D. Qian, "Color Retinal Image Enhancement Based on Luminosity and Contrast Adjustment," *IEEE Trans. Biomed. Eng.*, vol. 9294, no. c, pp. 1–1, 2017.

[3] K. Jin, M. Zhou, S. Wang, L. Lou, Y. Xu, J. Ye, and D. Qian, "Computer-aided diagnosis based on enhancement of degraded fundus photographs," *Acta Ophthalmol.*, no. 1994, pp. 1–7, 2017.

[4] L. Xiong, H. Li, and L. Xu, "An enhancement method for color retinal images based on image formation model," *Comput. Methods Programs Biomed.*, vol. 143, pp. 137–150, 2017.

[5] H. Singh, A. Kumar, L. K. Balyan, and G. K. Singh, "A novel optimally weighted framework of piecewise gamma corrected fractional order masking for satellite image enhancement," *Comput. Electr. Eng.*, pp. 1–17, 2017. doi 10.1016/j.compeleceng.2017.11.014.

[6] H. Singh, A. Kumar, L. K. Balyan, and G. K. Singh, "Swarm intelligence optimized piecewise gamma corrected histogram equalization for dark image enhancement," *Comput. Electr. Eng.*, pp. 1–14, 2017. doi:10.1016/j.compeleceng.2017.06.029.

[7] R. C. Gonzalez and R. E. Woods, *Digital Image Processing*, 4th ed. Pearson/Prentice-Hall, NY, 2017.

[8] K. Singh and R. Kapoor, "Image enhancement via Median-Mean Based Sub-Image-Clipped Histogram Equalization," *Optik -Int. J. Light and Electron Optics*, vol. 125, no. 17, pp. 4646-4651, Sept. 2014.

[9] S. C. F. Lin, C. Y. Wong, M. A. Rahman, G. Jiang, S . Liu, N. Kwok, H. Shi, Y.H. Yu and T. Wu, "Image enhancement using the averaging histogram equalization (AVHEQ) approach for contrast improvement and brightness Preservation," *Comput. and Elect. Eng.*, vol. 46, pp. 356-370, Aug. 2015.

[10] C. Y. Wong, G. Jiang, M. A. Rahman, S. Liu, S. C. F. Lin, N. Kwok, H. Shi, Y. H. Yu and T. Wu, "Histogram equalization and optimal profile compression based approach for colour image enhancement," *J. Visual Commun. and Image Represen.*, vol. 38, pp. 802-813, July 2016.

[11] C. Y. Wong, S. Liu, S. C. Liu, M. A. Rahman, S. C. F. Lin, G. Jiang, N. Kwok and H. Shi, "Image contrast enhancement using histogram equalization with maximum intensity coverage," *J. Modern Optics*, vol. 63, no. 16, pp. 1618-1629, Mar. 2016.

[12] S. C. Huang, F. C. Cheng and Y. S. Chiu, "Efficient Contrast Enhancement Using Adaptive Gamma Correction with Weighting Distribution," *IEEE Trans. Image Process*, vol. 22, no. 3, pp. 1032-1041, Mar. 2013.

[13] H. Singh, A. Kumar, L. K. Balyan, and G. K. Singh,"A novel optimally gamma corrected intensity span maximization approach for dark image enhancement,"*IEEE International Conference on Digital Signal Processing (DSP)*, London, United Kingdom, 2017, pp. 1-5. doi:10.1109/ICDSP.2017.8096035.

[14] H. Singh, N. Agrawal, A. Kumar, G. K. Singh and H. N. Lee, "A novel gamma correction approach using optimally clipped sub-equalization for dark image enhancement," *IEEE International Conference on Digital Signal Processing (DSP)*, Beijing, China, 2016, pp. 497-501.

[15] H. Singh and A. Kumar, "Satellite image enhancement using beta wavelet based gamma corrected adaptive knee transformation," *IEEE International Conference on Communication and Signal Processing (ICCSP)*, Melmaruvathur, India, 2016, pp. 128-132. doi: 10.1109/ICCSP.2016.7754552

[16] H. Singh, A. Kumar, L. K. Balyan and G. K. Singh, "Dark image enhancement using optimally compressed and equalized profile based parallel gamma correction," *2017 International Conference on Communication and Signal Processing (ICCSP)*, Chennai, India, 2017, pp. 1299-1303. doi: 10.1109/ICCSP.2017.8286592

[17] H. Singh, A. Kumar, L. K. Balyan and G. K. Singh, "Regionally equalized and contextually clipped gamma correction approach for dark image enhancement," *IEEE International Conference on Signal Processing and Integrated Networks (SPIN)*, Noida, India, 2017, pp. 431-436.

[18] S.C.F. Lin, C.Y. Wong, G. Jiang, M.A. Rahman, T.R. Ren, N. Kwok, H. Shi, Y. H. Yu and T. Wu, "Intensity and edge based adaptive unsharp masking filter for color image enhancement," *Optik–Int. J. for Light and Electron Optics*, vol. 127, no. 1, pp. 407-414, Jan. 2016.

[19] K. Singh, D. K. Vishwakarma, G. S. Walia, and R. Kapoor, "Contrast enhancement via texture region based histogram equalization," *J. Mod. Opt.*, vol. 63, no. 15, pp. 1444–1450, 2016.

[20] X.-S. Yang and S. Deb, "Cuckoo search via Lévy-flights," inProc. World Congr. Nature Biol. Inspired Comput., Dec. 2009, pp. 210–214.

[21] J. J. Staal, M. D. Abramoff, M. Niemeijer, M. A. Viergever, B. van Ginneken, "Ridge based vessel segmentation in color images of the retina", *IEEE Transactions on Medical Imaging*, 2004, vol. 23, pp. 501-509.